

## The Luusika potential field anomaly, eastern Estonia: modelling results

Marija Dmitrijeva<sup>a</sup>, Jüri Plado<sup>b</sup> and Tõnis Oja<sup>c</sup>

<sup>a</sup> School of Chemical Engineering, The University of Adelaide, SA 5005, Australia; [dmitrijeva.maria@gmail.com](mailto:dmitrijeva.maria@gmail.com)

<sup>b</sup> Institute of Ecology and Earth Sciences, University of Tartu, Ravila 14A, 50411 Tartu, Estonia; [juri.plado@ut.ee](mailto:juri.plado@ut.ee)

<sup>c</sup> Department of Geodesy, Estonian Land Board, Mustamäe tee 51, 10621 Tallinn, Estonia; [tonis.oja@maamet.ee](mailto:tonis.oja@maamet.ee)

Received 15 March 2018, accepted 30 July 2018, available online 13 November 2018

**Abstract.** This study considers the anomalous gravity and magnetic fields in the Alutaguse petrological–structural domain, eastern Estonia. A 10 km wide local maximum (+6.26 mGal) Bouguer anomaly field was discovered at 58.96°N, 26.61°E from the ground gravity data by the Estonian Land Board in 2010–2011. The ground magnetic field intensity measurements indicated a positive magnetic anomaly of 600 nT, in addition to the local gravity maximum. Based on depth estimations, the centre of the anomaly source is placed at 2500–3000 m within the ~1.8 to 1.9 Ga Svecofennian basement. To provide information on the physical properties of the causative source of the anomalies, the geophysical modelling of potential fields was carried out by testing a number of lithologies as sources. The lithologies considered were the known post-orogenic and anorogenic magmatic intrusions in the Estonian basement, as well as typical metamorphic rocks of the Alutaguse domain. The obtained models indicate that the Luusika feature has a range of densities from 2760 to 2920 kg/m<sup>3</sup> and magnetic susceptibilities from  $20\,000 \times 10^{-6}$  to  $56\,000 \times 10^{-6}$  SI. These models suggest that the Luusika causative source is an intermediate to the mafic rock unit, similar to post-orogenic or anorogenic massifs of the Svecofennian basement of Estonia.

**Key words:** potential fields, magnetic susceptibility, density, Estonia, geophysical modelling, Alutaguse domain.

### INTRODUCTION

The Precambrian crystalline basement of Estonia cannot be observed by conventional geological mapping as it is overlain by Neoproterozoic to Devonian sedimentary successions. Therefore, the Precambrian geology of Estonia is inferred from geophysical and predominantly magnetic data from approximately 500 deep drill holes (Puura et al. 1983). Based on the geophysical and geological observations, the Estonian basement within the Svecofennian orogenic domain has been divided (Koppelmaa 2002) into six petrological–structural domains: Alutaguse, Jõhvi, Tallinn, Tapa, West Estonian and South Estonian (Fig. 1). The structural domains are bordered by east–west striking Middle Estonian Fault Zones and the regional Paldiski–Pskov Deformational Zone, while showing gravity and magnetic lows in northern Estonia and high gravity and magnetic intensities in southern Estonia (Fig. 1; Soesoo et al. 2004; Kirs et al. 2009). Each petrological–structural domain is characterized by a specific assemblage of metamorphic rocks, petrophysical properties and distribution of metasediments and/or metavolcanites (Koistinen et al. 1996; Bogdanova et al. 2015). The domains also accommodate

widely distributed small- and middle-sized igneous intrusions associated with post-orogenic, i.e. postdating the Svecofennian orogeny, and anorogenic Palaeo-Mesoproterozoic Rapakivi Province magmatism (Koistinen et al. 1996). The intrusions are usually accompanied by geophysical anomalies, e.g. the 1833 Ma post-orogenic Taadikvere massif, and some of the felsic rapakivi and related mafic rock intrusions: Märjamaa, Naissaare, Neeme, Abja and Sigula, which belong to the 1620–1650 Ma Wiborg rapakivi subprovince (Laitakari et al. 1996).

Extensive geophysical mapping of Estonia, carried out in the 1960s–1980s (e.g. Maasik & Sildvee 1965; Gromov 1993), resulted in maps of magnetic and gravity fields of various scales and coverage. Nevertheless, some areas of Estonia remained unmapped because of insufficient geophysical measurements. This applies to the Luusika region in eastern Estonia, which is located beyond the dense grid of the gravity measurements (e.g. Ellmann et al. 2009) and is not fully covered by aeromagnetic data (Fig. 2; Melitskaya & Papko 1992).

A single positive peak with an amplitude of about 6.3 mGal in the Bouguer anomaly field was discovered

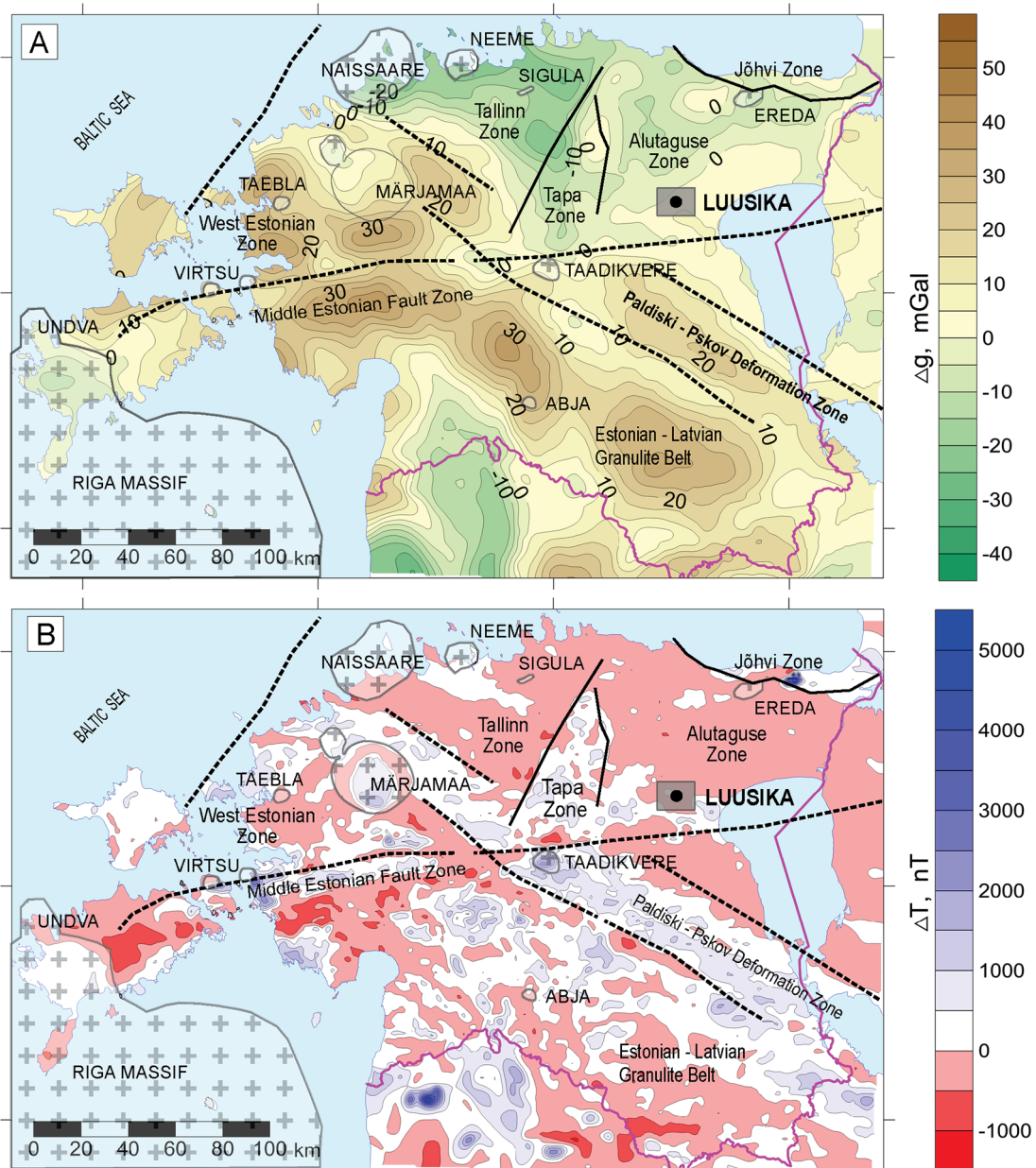


**Fig. 1.** Structural features and metamorphic complexes of the Precambrian basement compared to (A) Bouguer gravity and (B) magnetic anomaly maps. Non-marked areas represent Svecofennian metamorphic and plutonic rocks; crossed areas are anorogenic complexes of rapakivi and related granites. Geological data are after Puura et al. (1997) and Bogdanova et al. (2015). Geophysical overview maps are by the Geological Survey of Estonia. The grey square indicates the location of the studied Luusika area.

in 2011 by the Estonian Land Board (Oja 2011) in the Luusika region. The Bouguer anomaly contours display an elliptical gravity anomaly, with dimensions of about  $12 \text{ km} \times 10 \text{ km}$  (Fig. 2). The Luusika Bouguer anomaly source is placed within the Alutaguse domain, which is characterized by amphibolite facies rocks that pass towards granulite facies rocks (Bogdanova et al. 2015). The Alutaguse domain consists of metamorphosed

turbidites, pyroxene gneisses, pyroxene-bearing calc-silicate rocks, marbles and quartzites, as well as intrusive rocks (gabbros and granites) and migmatites (Koppelmaa 2002). The domain represents a deformed and strongly folded marginal part of the sedimentary basin that extends to St Petersburg and Novgorod (Bogdanova et al. 2015). Based on petrophysical measurements of a few hundred drill core samples from the Alutaguse

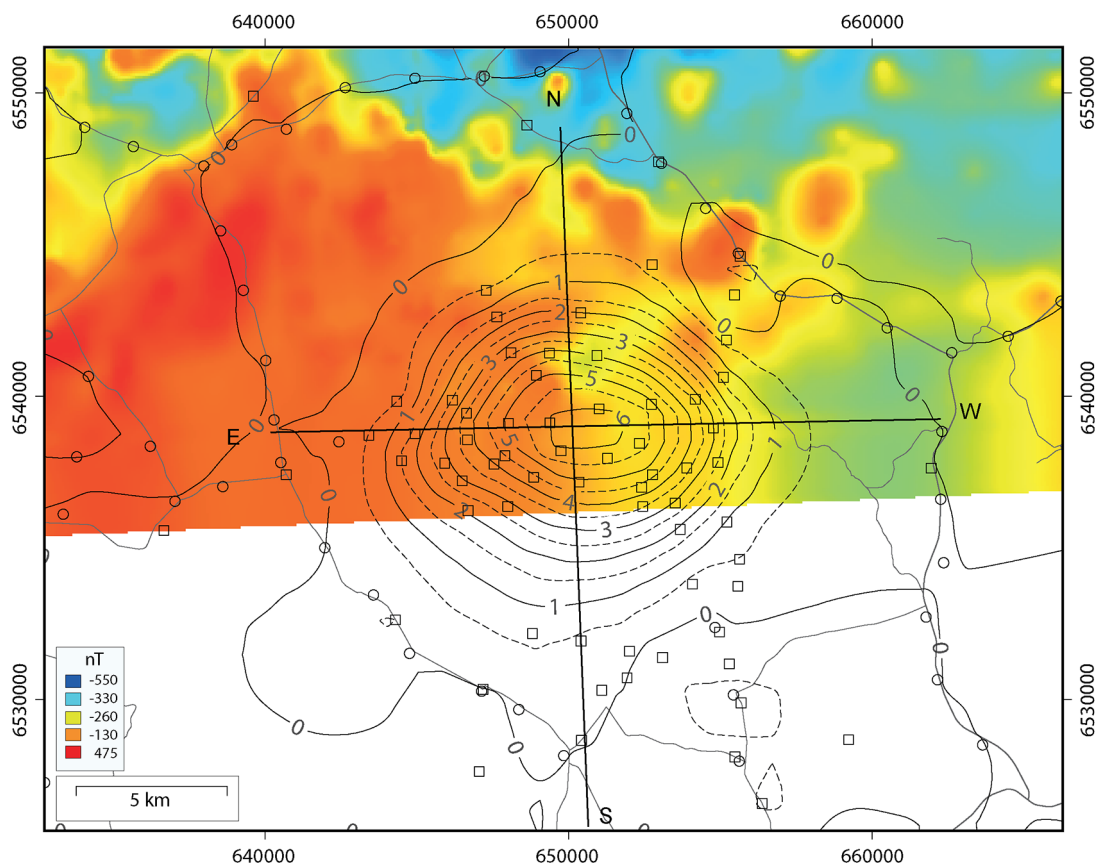


**Fig. 2.** Aeromagnetic map (1:25 000, Melitskaya & Papko 1992) covering the northern part of the Luusika area but without resolving a magnetic field anomaly; the gravity (Bouguer) local anomaly contours after Oja (2011) in the Luusika area; gravity points measured before 2010 (along the road network shown in the background) and in 2010–2011 are marked with circles and squares, respectively. The Estonian L-EST97 coordinate system is used for map projection.

domain, the density and magnetic susceptibility of the rocks range from 2540 to 2890 kg/m<sup>3</sup>, and from  $10 \times 10^{-6}$  to  $2010 \times 10^{-6}$  SI, respectively (Puura et al. 1983), with a mean of 2680 kg/m<sup>3</sup> and  $138 \times 10^{-6}$  SI. These values are low in comparison with densities and magnetic susceptibilities from other Estonian crystalline domains (fig. 21 in Puura et al. 1983).

As there are no deep drill holes in the proximity of the Luusika anomaly, the gravity and magnetic data sets are the only existing pieces of information about the anomaly. In this study we present the results from field work and direct modelling in and around the Luusika anomaly to describe the causative source. The primary objective is to specify the magnetic field intensity over the Luusika gravity anomaly and to provide information on the physical properties of the source body by means of iterative direct modelling of potential fields. For that purpose we simulated bodies with physical properties similar to lithologies within the Alutaguse domain, and the known post-orogenic and anorogenic intrusions

within the Estonian crystalline basement. Finally, we discuss the petrophysical properties of the Luusika causative source and propose its origin.

## METHODS AND DATA

### Gravity data processing

The geophysical data sets used to model the petrophysical properties of the geological body underlying the Luusika anomaly include the gravity data collected in 2010–2011, the residual Bouguer anomaly values calculated by the Estonian Land Board (Oja 2011) and the ground-based magnetic data obtained in 2014 by the present authors. The gravity values with corresponding coordinates and height at every survey site (altogether 71 points, Fig. 2) were measured using the relative CG-5 gravimeter (Scintrex Ltd) and the geodetic GNSS receiver (Trimble 5800) combined with the network RTK (real-time kinematic) service. The gravity survey points were

connected to the 3rd-order points of the Estonian gravity network where gravity acceleration values with an uncertainty of  $\pm 0.05$  mGal are known in the national gravity system GV-EST95, based on the absolute gravity measurements (Ellmann et al 2009; Oja 2012). After correcting the gravity readings for the tides and the instrument's height and drift, an uncertainty of 0.10 mGal for the gravity data was estimated. The combined uncertainty of 0.15 m for the coordinates and height (in the national geodetic frame EUREF-EST97) includes the conversion error from the geodetic height to the normal height in BHS77 (Baltic height system 1977) by using the national EST-GEOID2011 model (Ellmann et al. 2011). For more details about the national gravity network, the measurement and data processing techniques, see Ellmann et al. (2009), Oja et al. (2011) and Oja (2012).

The Bouguer anomaly was computed using the density of  $2300 \text{ kg/m}^3$  on the GRS80 ellipsoid. The regular grid of gravity anomalies was computed with continuous curvature splines with the tension factor of 0.25 (Smith & Wessel 1990). Two different grids were calculated for the area  $58.85\text{--}59.07^\circ\text{N}$  and  $26.30\text{--}26.90^\circ\text{E}$  (Fig. 2). The computation of the first grid includes 118 gravity data points measured within the grid area before 2010 and in 2010–2011. For the second grid, only gravity points measured before 2010 (47 points) were used in computation. The second grid approximates the regional trend since no survey points (squares in Fig. 2) are found over the area with a local maximum in the Bouguer anomaly field. The resultant residual Bouguer anomaly was obtained by subtracting the first grid from the second one. The result, a residual gravity anomaly ranging from  $-0.8$  to  $6.3$  mGal in amplitude (contours in Fig. 2), was used as the basis for this study.

### Magnetic data acquisition and processing

Ground magnetic measurements in the Luusika area were carried out in 2014, relying on two (stationary and mobile) independently working time-synchronized model G-856 proton precession magnetometers (Geomatrix). The mobile magnetometer was carried by two people equipped with a hand-held GPS device. Individual measurements of the magnetic field intensity were performed every 100 m along five north–south and two east–west striking profiles along forest roads and division lines between compartments (see Fig. 3B for location) tied with location coordinates. The position and extension of the profiles were chosen to extend the limit of the gravity anomaly. The stationary magnetometer was installed in the study area to record diurnal variations in the geomagnetic field at every 300 s during the field-work period. The ground survey readings were

corrected against the base-station readings. This was necessary since during a field campaign in 2014, the magnitudes of diurnal variations were found to be as high as 50 nT. Lastly, the magnetic anomaly map was created by the minimum curvature method (Smith & Wessel 1990).

### Direct modelling

The depth estimations of the underlying geological body were carried out based on the gravity anomaly. Calculations were made along two north–south and west–east profiles (Fig. 2) by applying the half-width and gradient-amplitude ratio methods to the gravity profiles (Smith 1959, 1960; Sharma 1976). Various geometric shapes of the possible anomaly source were considered: sphere, horizontal and vertical cylinder and a tilted elliptic pipe.

Successive direct geophysical modelling combining both gravity and magnetic data was performed using the previously described depth estimations. The density and magnetic susceptibility of the background were set to  $2680 \text{ kg/m}^3$  and  $138 \times 10^{-6}$  SI, respectively, thus corresponding to the averages of the Alutaguse domain. The direct modelling was performed based on the gravity and magnetic response curves, along two orthogonal north–south and west–east profiles (see Fig. 3A; B for location). The models were 3-dimensional, each consisting of an elliptic pipe with vertical axis and 12 vertical sides (Fig. 4). By changing the vertical and horizontal dimensions of the pipe, we tried to match the model curves to fit the observed data by trial-and-error.

The direct modelling considered gravity and magnetic anomalies separately. Several models were composed, each with physical properties attributed to the specific lithologies in the Estonian crystalline basement (Table 1). The vertical extent and depth to the top of the magnetic models were kept equal to the gravity models. For the magnetic models, the International Geomagnetic Reference Field parameters for the Luusika area in 2014 were used (field intensity  $F = 51\,888$  nT, inclination  $I = 72.8^\circ$  and declination  $D = 8.5^\circ$ ). The petrophysical properties of lithologies, Koenigsberger ratio ( $Q$ ) and direction of the remanent magnetization were introduced. As there exist no palaeomagnetic data of oriented drill cores from the Estonian crystalline basement, we used the values of declination ( $D$ ) and inclination ( $I$ ) derived from Pesonen et al. (1989) for  $\sim 1.88$  and  $\sim 1.6$  Ga.

It is nevertheless important to highlight that during the interpretation of potential field data, the ‘source’ is determined by the ‘effect’. This problem has no unique solution, as for a given distribution of gravity/magnetic

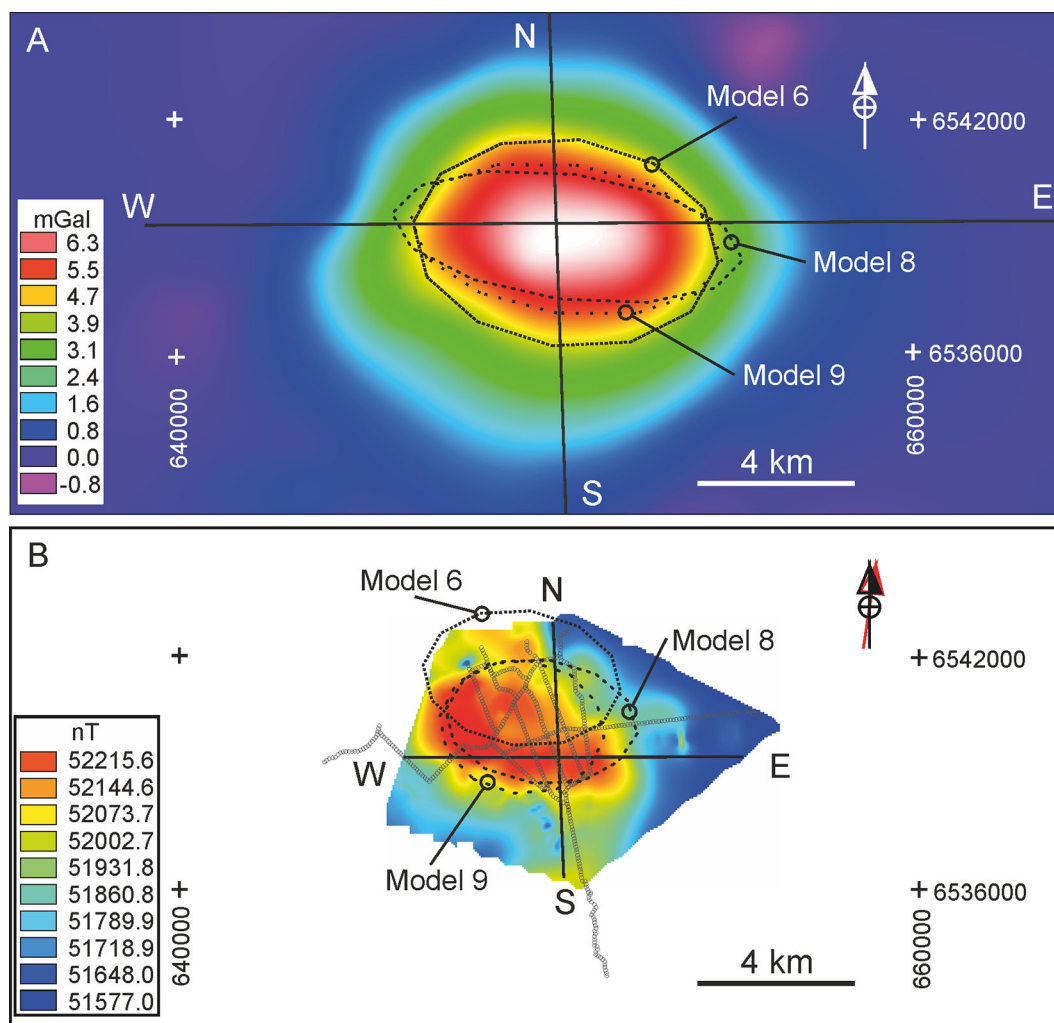


**Fig. 3.** Residual gravity anomaly map (A) and the total magnetic intensity map over the Luusika area (B) with the location of the north–south and west–east profiles; (B) also features the position of ground-based magnetic survey points. Outlines of models are given.

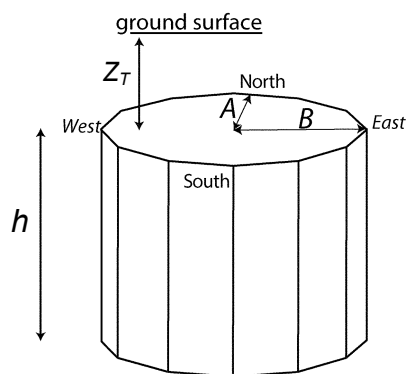


**Fig. 4.** Modelled geological bodies represented by elliptic pipes. Semi-axes  $A$  and  $B$  refer to body’s lateral extension in north–south and east–west directions. The parameter  $h$  characterizes the vertical extension of the pipe and  $z_T$  refers to the depth to the top of the model.

anomalies, an infinite number of mass/magnetization distributions can be found which would produce the same anomaly.

## RESULTS

### Magnetic field

The ground total magnetic intensity map (Fig. 3B) indicates the presence of an ellipsoid-shaped magnetic anomaly in the Luusika region, with the amplitude of about 600 nT. It is most likely that magnetic anomaly results from an anomalously high magnetization of the underlying Luusika body compared to its surroundings. The magnetic anomaly has an elongated (in NW–SE direction) elliptic shape of 5.0 km × 2.5 km (Fig. 3),

**Table 1.** Model physical properties and modelling results

Model No.	$\rho$ (kg/m <sup>3</sup> )	Status 1	Dimensions		$\kappa$ ×10 <sup>-6</sup> SI	$Q$	$D$ (°)	$I$ (°)	Status 2	Rock type/ location
			$z_T$ (m)	$h$ (m)						
Alutaguse domain										
1	2820	Accept	1500	5500	300	1.0	326	30	Reject	Gabbro
2	2870	Accept	1500	3000	2350	2.4	326	30	Reject	Marble
3	2850	Accept	1500	3000	3900	6.3	326	30	Reject	Gneiss
4	3320	Reject			7000	22.0				Pyroxene-bearing calc-silicate
5	2700	Reject			1700	13.9				Quartzite
Estonian post-orogenic plutons										
6	2760	Accept	600	5500	20 000	0.91	352	17	Accept	Taadikvere quartz monzonite
7	2740	Reject			54 000	3.6				Virtsu quartz monzonite
Estonian anorogenic plutons										
8	2920	Accept	1800	3000	56 000	0.46	352	17	Accept	Abja quartz monzodiorite
9	2890	Accept	1500	3000	32 000	0.91	326	30	Accept	Sigula gabbro-diorite
10	2810	Accept	1150	3500	11 800	1.04	352	17	Reject	Riga plagioclase porphyry
11	2720	Reject			30 000	0.12				Märjamaa rapakivi granite I phase

Status indicates a successful (Accept) or unsuccessful (Reject) model after the gravity (Status 1) and magnetic (Status 2) analyses;  $\rho$  = density;  $z_T$  = depth to the top of the model;  $h$  = vertical extent of the model (Fig. 4);  $Q$  = Koenigsberger ratio;  $D$  and  $I$  = declination and inclination of the natural remanent magnetization, respectively.

which is smaller than the gravity anomaly. The magnetic anomaly is located towards the NW of the gravity maximum. Being located on the eastern edge of the regional positive anomaly, the Luusika anomaly cannot be seen in the aeromagnetic map (Fig. 2). This is mostly due to the differences between the magnetic fields at the eastern edge of the Luusika anomaly. The ground magnetic map shows a sharp decrease in values towards the east, while the aeromagnetic map does not. This may either be due to (i) regional (deeper) features in the aeromagnetic map that obscure the Luusika ground magnetic anomaly or to (ii) different data treatment procedures.

### Depth estimations

The depth estimations were based on residual Bouguer anomaly data. The maximum amplitude ( $A_{\max}$ ) of the residual anomaly in the Luusika area reaches 6.26 mGal. The anomaly half-width values ( $x_{1/2}$ ) at half-amplitude were measured to be 4050 m for the east–west and 2850 m for the north–south profile. Assuming a simple geometric body (sphere, horizontal cylinder or tilted elliptic pipe), the depth to the centre of the body was

estimated to be between 2000 and 4200 m, with a mean of 2500 m. The gradient-amplitude method (Smith 1959, 1960; Sharma 1976) resulted in depths between 1650 and 5400 m, with a mean of 3000 m. Thus, both depth methods point to a source of the Luusika anomaly located within the crystalline basement since the overlying sediment thickness is approximately 200 m in the Luusika area.

### Gravity models

In order to produce a positive gravity anomaly, the causative source must have a reasonable positive density contrast with surrounding rocks. The physical properties of the models (Koppelmaa 2002; All et al. 2004; Table 1) are constrained by those of various rock types in the Estonian crystalline basement. In the first attempt, eleven gravity models were composed. Four of the models were rejected on the basis of unsuccessful modelling results due to the poor fit between the calculated and observed curves (Status 1 in Table 1). The vertical extent ( $h$ ) of the model was altered, but the centre of the model remained between 2250 and 3000 m in accordance with depth estimations. Densities below

2680 kg/m<sup>3</sup>, which would produce negative anomalies, thus, contradicting the observations, were rejected. Densities below 2760 kg/m<sup>3</sup> would need models that overlap the sedimentary cover and were rejected as well. The best match of the calculated and observed curves was achieved when the geological model had a density value within the interval from 2760 to 2920 kg/m<sup>3</sup>. The top surface of the elliptic pipes was placed to a depth ( $z_T$ ) of 600 to 1800 m (Table 1).

### Magnetic models

Analogously to gravity modelling, the same, but shorter perpendicular east–west and north–south profiles were investigated (Fig. 3B). In the east–west profile, the anomaly is asymmetrical and the central part is represented by a plateau-like magnetic low combined with maximum peaks on the eastern and western sides of the profiles (Fig. 5). In the north–south profile, the

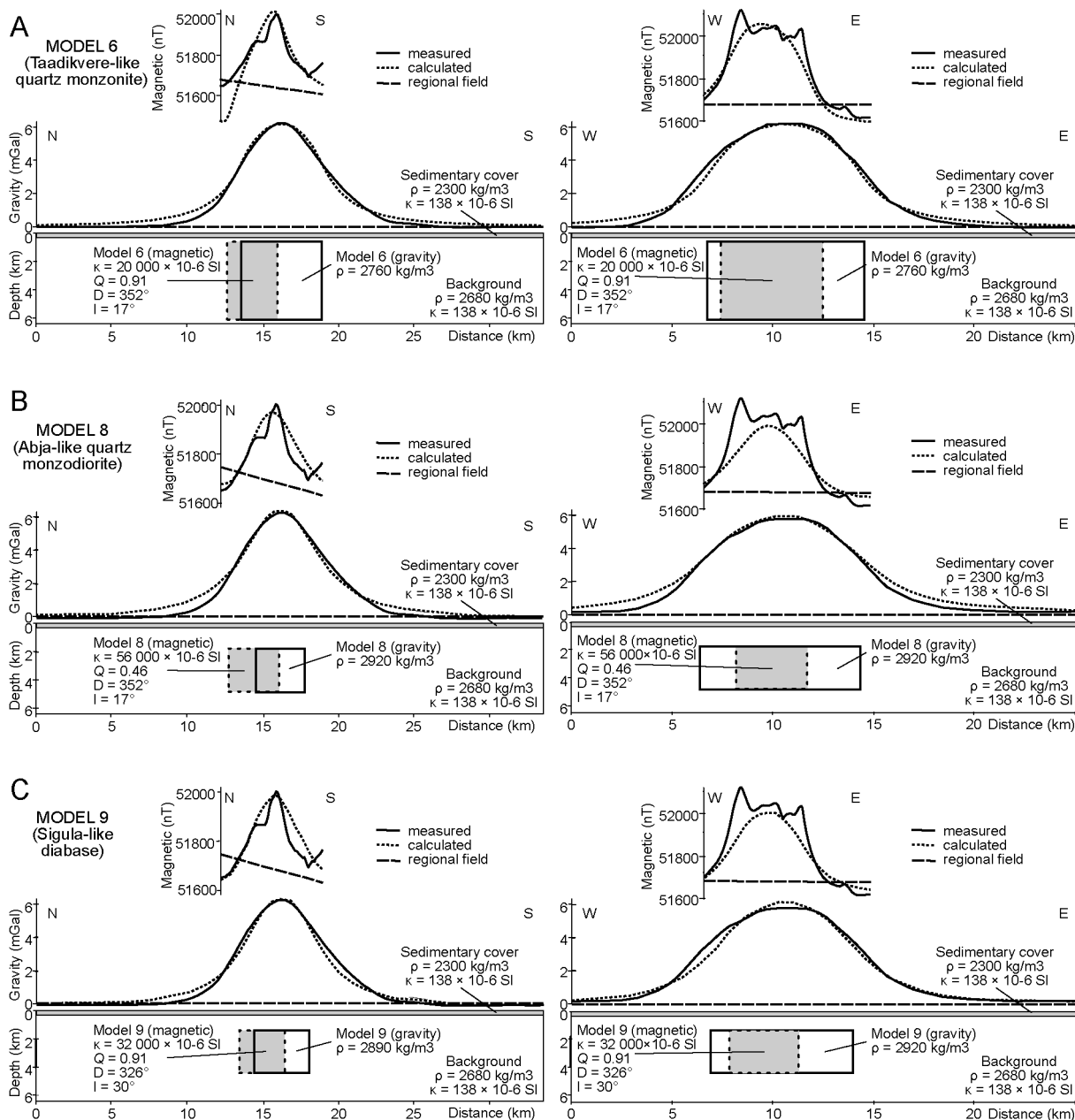


**Fig. 5.** Magnetic and gravity models 6 (A), 8 (B) and 9 (C) (Table 1). The left side represents the north–south-oriented, the right side east–west-oriented profile, respectively. Every model (bottom subfigure) includes magnetic (top subfigure) and gravity (middle subfigure) profile data providing information on measured, calculated and regional trends.

magnetic field is characterized by a unimodal peak with asymmetrical slopes, featuring a tiny kink on the northern side of the profiles. In total, seven models were composed based on magnetic data, from which four were rejected because of a poor fit (Status 2 in Table 1).

The lowest magnetic susceptibility values in the Alutaguse domain lithologies range between  $300 \times 10^{-6}$  and  $1800 \times 10^{-6}$  SI. Calculated magnetic responses of these values were very weak compared to the measured data and, as a result, models 1–3 and 10 were rejected (Table 1). The magnetic susceptibilities and remanences of Estonian post-orogenic and anorogenic lithologies are significantly higher compared to the Alutaguse domain lithologies, varying between  $11\,800 \times 10^{-6}$  and  $56\,000 \times 10^{-6}$  SI. By modifying magnetic susceptibility values, a reasonable overlap of calculated and observed magnetic fields was achieved for physical properties that resemble those of the Taadikvere quartz monzonite, Abja quartz monzodiorite and Sigula gabbro-diabase intrusions (models 6, 8 and 9 in Table 1 and Fig. 5).

## DISCUSSION

The gravity and magnetic anomalies are caused by physical properties (such as density and magnetization), location, geometry and volume of an anomalous body in the crystalline basement, which deviate from those of the surrounding rock. In the Luusika area, the Bouguer gravity and ground-based magnetic field data show positive anomalies which are clearly associated with a denser and more magnetically anomalous rock unit compared to the Alutaguse mica gneisses prevailing in the area.

In all the models, the magnetic anomaly and its geological source are smaller and located north to northwest of the centre of the gravity anomaly. The gravity and magnetic anomalies do not coincide, suggesting that either the Luusika feature is not homogeneous, and its denser mass is not necessarily more magnetic, or this mismatch occurs due to the vector magnetization effect. By this reasoning, the modelling of gravity and magnetic fields by an identical body for both failed.

The interpretation of the gravity and magnetic field anomalies is, nevertheless, ambiguous as any anomaly could be caused by an infinite number of possible sources. Although the anomaly of a given body may be calculated uniquely, there are always a number of bodies that could give rise to the specified anomaly. Using, however, the lithological and petrophysical data of the Estonian basement rocks as constraining values, we are able to propose eleven igneous and metamorphic rock types to represent the causative source. Based on

the geological, structural (sediment cover thickness) and petrophysical information available, and the modelling results, we decreased the ambiguity by rejecting eight of these possible scenarios (Table 1). The other three intrusional scenarios, however, do not provide a unique solution for the origin of the causative body of the Luusika potential field anomaly. The geometry of the Luusika Bouguer anomaly refers to an undeformed elliptical body with a lateral extension from 5 to 8 km (Fig. 5). The lateral extension of the magnetic anomaly source is somewhat less, being between 3 and 5 km. According to the modelling results and geological/geochronological knowledge of the Estonian basement, the Luusika body may belong to the Svecofennian post-orogenic rock group or the mafic satellite of the anorogenic Wiborg rapakivi suite.

Out of all simulated rock types, the Taadikvere post-orogenic quartz monzonitic intrusion is petrophysically the one that shows the greatest similarities to the Luusika body (Figs 1 and 4). Similarly to Taadikvere, Luusika is located close to the east–west-striking Middle Estonian Fault Zone, which formed in a brittle crust environment predating the rapakivi event (Puura & Flodén 2000). The Taadikvere quartz monzonite intrusion contains anomalously large amounts of ore and the accessory minerals hornblende, apatite (1–2%) and titanomagnetite (2–5%) (Niin 1997), which could cause or contribute to the observed potential field signature.

On the other hand, anorogenic intrusions are in the same way possible candidates for the Luusika potential field anomalies source since the magmatic mafic series of monzodiorite, gabbros, dolerite dykes and sills are closely associated with felsic rapakivi plutons (Laitakari et al. 1996). The Sigula fault-related dyke-like gabbro-diabase is located in the Tallinn domain and the ellipse-shaped Abja quartz monzodiorite lies within the southern Estonian granulite domain (Fig. 1; Soesoo et al. 2004). Both intrusions are mafic and have the highest densities amongst all the simulated rock types (Table 1). They are also characterized by positive gravity anomalies of 1.5 mGal (Sigula) and 2.5 mGal (Abja) (Petersell et al. 1985). The Sigula gabbro-diabase intrusion appears also as a local positive anomaly on the magnetic map (Koppelmaa & Kivisilla 1998). Abja and Sigula, with a susceptibility of  $\bar{\chi} = 24\,000 \times 10^{-6}$  SI and  $\bar{\chi} = 56\,000 \times 10^{-6}$  SI, respectively, have considerably higher magnetic susceptibilities compared to the hosting Alutaguse domain and, as a result, produced plausible models.

The obtained models of simulated rock types of the post-orogenic Taadikvere and anorogenic Abja and Sigula-like lithologies produced the best-matched models for the Luusika potential field anomaly as their density and magnetic susceptibility are comparable to

those of the Luusika source body. We therefore propose a Taadikvere-like quartz monzonite intrusion as a likely origin of the Luusika body due to the petrophysical similarities; however, the exact rock type and origin can be confirmed by direct drilling only.

## CONCLUSIONS

This study provides a geological insight into the recently discovered Luusika potential field anomalies in eastern Estonia. The investigation of coexisting gravity and magnetic anomalies revealed that the causative source of the anomalies is a denser and more magnetic rock body than the metasedimentary host rocks in the Alutaguse domain, with its centre located at depths between 2500 and 3000 m. The modelling revealed that the density of the Luusika causative source was in a range of 2760–2929 kg/m<sup>3</sup>, while magnetic susceptibility had to correspond to a range of  $20\,000 \times 10^{-6}$  to  $56\,000 \times 10^{-6}$  SI. Therefore, the Luusika body is an anomaly within the metasedimentary Alutaguse domain and a likely representative of an intrusive quartz monzodiorite or gabbro-diorite unit.

The step-wise gravity and magnetic modelling, and use of petrophysical properties of intermediate to mafic post-orogenic (Taadikvere quartz monzonite) and anorogenic intrusions (Sigula gabbro-diorite and Abja quartz monzodiorite), resulted in best-matched models for the Luusika potential field anomaly as their density and magnetic susceptibility are comparable to those of the Luusika source body. The modelling and comparison of petrophysical properties of the lithologies suggest that the Luusika causative source represents an intermediate to mafic rock by composition, similar to the Abja, Sigula or Taadikvere plutons.

**Acknowledgements.** We thank former students of the Department of Geology, University of Tartu, and Argo Jõelet for help provided during field-work. The manuscript significantly benefited from the comments of the reviewers Krister Sundblad and Lauri J. Pesonen. We are grateful to Liam Courtney-Davies for language editing and proofreading. The work by Jüri Plado was supported by the Estonian Research Council project IUT20-34. The publication costs of this article were partially covered by the Estonian Academy of Sciences.

## REFERENCES

All, T., Puura, V. & Vaher, R. 2004. Orogenic structures of the Precambrian basement of Estonia as revealed from the integrated modelling of the crust. *Proceedings of the Estonian Academy of Sciences, Geology*, **53**, 165–189.

- Bogdanova, S., Gorbachev, R., Skridlaite, G., Soesoo, A., Taran, L. & Kurlovich, D. 2015. Trans-Baltic Palaeoproterozoic correlations towards the reconstruction of supercontinent Columbia/Nuna. *Precambrian Research*, **259**, 5–33.
- Ellmann, A., All, T. & Oja, T. 2009. Towards unification of terrestrial gravity data sets in Estonia. *Estonian Journal of Earth Sciences*, **58**, 229–245.
- Ellmann, A., Oja, T. & Jürgenson, H. 2011. Application of space technologies to improve geoid and gravity field models over Estonia. *Geodet*, **41**, 22–25 [in Estonian].
- Gromov, O. 1993. *Sostavlenie gravimetricheskikh kart m-ba 1:50 000 i 1:200 000 i magnitometricheskoy karty m-ba 1:200 000 Severo-vostochnoj Éstonii [Report on Gravimetric (1:50 000) and Magnetic (1:200 000) Mapping of Northeastern Estonia]*. Geological Survey of Estonia, Tallinn, 67 pp. [in Russian].
- Kirs, J., Puura, V., Soesoo, A., Klein, V., Konsa, M., Koppelmaa, H., Niin, M. & Urtson, K. 2009. The crystalline basement of Estonia: rock complexes of the Palaeoproterozoic Orosirian and Statherian and Mesoproterozoic Calymmian periods, and regional correlations. *Estonian Journal of Earth Sciences*, **58**, 219–228.
- Koistinen, T., Klein, V., Koppelmaa, H., Korsman, K., Lahtinen, R., Nironen, M., Puura, V., Saltikova, T., Tikhomirov, S. & Yanovskiy, A. 1996. Paleoproterozoic Svecofennian orogenic belt in the surroundings of the Gulf of Finland. In *Explanation to the Map of Precambrian Basement of the Gulf of Finland and Surrounding Area 1:1 Million* (Koistinen, T., ed.), *Geological Survey of Finland, Special Paper*, **21**, 21–57.
- Koppelmaa, H. 2002. *Geological Map of the Crystalline Basement of Estonia. Scale 1:400 000. Explanation to the Map Estonian Version*. Geological Survey of Estonia, Tallinn, 32 pp. [in Estonian].
- Koppelmaa, H. & Kivisilla, J. 1998. *Geological Map of the Crystalline Basement of Northern Estonia. Scale 1:200 000. Explanation to the Map*. Geological Survey of Estonia, Tallinn, 33 pp.
- Laitakari, I., Rämö, T., Suominen, V., Niin, M., Stepanov, K. & Amantov, A. 1996. Subjotnian: rapakivi granites and related rocks in the surroundings of the Gulf of Finland. In *Explanation to the Map of Precambrian Basement of the Gulf of Finland and Surrounding Area 1:1 Million* (Koistinen, T., ed.), *Geological Survey of Finland, Special Paper*, **21**, 59–97.
- Maasik, V. & Sildvee, H. 1965. *Eesti NSV territooriumi maakoore vertikaal-liikumiste uurimine gravimeetrilise meetodiga [The Study of Vertical Movements of the Crust of the Estonian SSR Territory by the Gravimetric Method]*. Geological Survey of Estonia, Tallinn, 17 pp. [in Estonian].
- Melitskaya, V. I. & Papko, A. M. 1992. *Otchet o rezul'tatakh aeromagnitnoj s'emki masshtabov 1:25 000, 1:50 000 na territorii Éstonii i prilégayushchego shelfa, provedennoj partiei nr. 49 v 1987–1991 gg. [The Results of Aeromagnetic Mapping by Working Group No. 49 at Scales of 1:25 000 and 1:50 000 on Estonian Territory 1987–1991. Report of Investigation]*. Geological Survey of Belarus, Minsk, 75 pp. [in Russian].

- Niin, M. 1997. Svecofennian granitoids of the crystalline basement of Estonia; classification on the basis of geological structure, mineral and chemical composition. *Bulletin of the Geological Survey of Estonia*, **7**, 4–40.
- Oja, T. 2011. The uplift of the gravity anomaly field near Luusika and its impact on geoid. *Geodeet*, **41**, 26–30 [in Estonian].
- Oja, T. 2012. Gravity system and network in Estonia. In *Geodesy for Planet Earth, Proceedings of the IAG2009* (Kenyon, S., Pacino, M. C. & Marti, U., eds), *International Association of Geodesy Symposia*, **136**, 315–322.
- Oja, T., Türk, K., Ellmann, A., Gruno, A., Bloom, A. & Sulaoja, M. 2011. Relative gravity surveys on ice-covered water bodies. In *Environmental Engineering, The 8th International Conference, May 19–20, 2011, Vilnius*, pp. 1394–1401.
- Pesonen, L. J., Torsvik, T. H., Elming, S.-Å. & Bylund, G. 1989. Crustal evolution of Fennoscandia – palaeo-magnetic constrains. *Tectonophysics*, **162**, 27–49.
- Petersell, V., Talpas, A. & Pöldvere, A. 1985. *Otchet ob izuchenii zhelezorudnykh formatsii v dokembrii Éstonii* [An Investigation of Iron Ore Formations in the Precambrian of Estonia]. Geological Survey of Estonia, Tallinn, 129 pp. [in Russian].
- Puura, V. & Flodén, T. 2000. Rapakivi-related basement structures in the Baltic Sea area; a regional approach. *GFF*, **122**, 257–272.
- Puura, V., Klein, V., Koppelmaa, H. & Niin, M. 1997. Precambrian Basement. In *Geology and Mineral Resources of Estonia* (Raukas, A. & Teedumäe, A., eds), pp. 27–34. Estonian Academy Publishers, Tallinn.
- Puura, V., Vaher, R., Klein, V., Koppelmaa, H., Niin, M., Vanamb, V. & Kirs, J. 1983. *Kristallicheskij fundament Éstonii* [The Crystalline Basement of Estonian Territory]. Nauka, Moscow, 208 pp. [in Russian, with extended English summary].
- Sharma, P. V. 1976. *Geophysical Methods in Geology*. Elsevier, Amsterdam, 428 pp.
- Smith, R. A. 1959. Some depth formulae for local magnetic and gravity anomalies. *Geophysical Prospecting*, **7**, 55–63.
- Smith, R. A. 1960. Some formulae for interpreting local gravity anomalies. *Geophysical Prospecting*, **8**, 607–613.
- Smith, W. H. F. & Wessel, P. 1990. Gridding with continuous curvature splines in tension. *Geophysics*, **55**, 293–305.
- Soesoo, A., Puura, V., Kirs, J., Petersell, V., Niin, M. & All, T. 2004. Outlines of the Precambrian basement of Estonia. *Proceedings of the Estonian Academy of Sciences, Geology*, **53**, 149–164.

## Luusika gravitatsiooni- ja magnetvälja anomaalia uuringud Ida-Eestis

Marija Dmitrijeva, Jüri Plado ja Tõnis Oja

On käsitletud positiivset raskuskiirenduse ja magnetvälja anomaaliat Luusika piirkonnas, mis paikneb Alutaguse struktuur-fatsiaalses vööndis Ida-Eestis. Luusika piirkonda iseloomustab  $10 \times 12$  km suurune kerge gravitatsiooniväli maksimaalse amplituudiga +6,26 mGal, mis esineb koos magnetvälja positiivse anomaaliaga amplituudiga kuni 600 nT. Kasutades raskuskiirenduse (Bouguer) anomaalia iseloomustamisel gradient-amplituudi- ja poollaiusemeetodit, määrati anomaaliaallika keskme sügavuseks 2500–3000 m. Eesti kristalses aluskorras leiduvate kivimite teadaolevate füüsikaliste omaduste alusel modelleeriti Luusika anomaaliat. Modelleerimise tulemusel leiti: 1) anomaaliat põhjustava keha tihedus jääb vahemikku 2760–2920 kg/m<sup>3</sup>, 2) magnetilise vastuvõtlikkuse väärtus on taustkivimiga võrreldes väga suur ( $20\,000$  kuni  $56\,000 \times 10^{-6}$  SI). Mudelid kinnitavad analoogia alusel, et Luusika keha sarnaneb Abja, Sigula ja Taadikvere massiividega.